УДК 621.384.6.01

O.I. Girka[1], I.O. Bizyukov[1], O.A. Bizyukov[1], K.M. Sereda[1], O.V. Romashchenko[2]
[1] V.N. Karazin Kharkiv National University, 61022, Kharkiv, Svobody Sq., 4, Ukraine
e-mail: alexxxgir@gmail.com
[2] Volodymyr Dahl East Ukrainian National University, 91034, Luhansk, Molodizhny Bl., 20a

FOCUSED ION SOURCE FOR THE MICROELECTRONICS THIN FILMS PROCESSING

This paper presents the results of the optimized compact ion source application for the corrective ion-beam etching with the purpose to regulate the thickness and uniformity of microelectronics functional layers with high precision on large-diameter wafers. The functional layers on the wafers are etched by the scanning ion beam. Localization and power of the beam correspond to the thin film surface inhomogeneity. The possibility of both correcting the thin film surface inhomogeneity and increasing the surface roughness with the precision up to *4 Å* is shown.
Key words: compact ion source, film surface inhomogeneity, ion-beam etching.

Introduction

Further development of plasma technologies is focused on improving the critical parameters of the ion and plasma sources. One of them is density of the ion beam current, which can be achieved through the increasing the ion current and/or improving the focusing of the ion flux. Recently reviewed duoplasmatron designs are capable to produce ion beams [1] using the focusing of the diverged ion beams by Einsel lens and the efforts are focused on increasing the total current of the ion beam. Cold-cathode filamentless gridless compact ion source described in this paper is able to provide the hydrogen ion beam with the current density of 0.16 A/cm^2 typical for fusion devices and should allow the appropriate experimental modelling of plasma-wall interaction.

Recently, the particular attention has been paid to the anode layer ion beam source (this kind of sources is usually referred to as Hall thrusters [2]), which produces cylindrical ion beam with the current up to 300 mA. It is characterized by simple and robust design, stability of the operation, portability. The most important parameter of this kind of sources is the highest ratio of the ion beam current to the discharge current. It is possible to extract 40÷80% of the discharge current and convert it to the ion beam current. (For comparison, the Duoplasmatron ion source is capable to extract only up to 1÷3% of the discharge current).

Therefore, it is very attractive to design a modified version of the anode layer ion source, which can produce focused ion beam with extremely high ion beam current density, but preserving the main advantages of this type of ion sources. The basic principal design of the modified ion source (FALCON) has been recently patented [3]. Further development of the FALCON ion source was described in [4], where theoretical and experimental investigations of ion beam formation via application of ballistic and magnetic focusing were investigated.

In this paper, a set of investigations is carried out to optimize the Hall thruster focusing system for production and treatment of microelectronics functional layers. The deviations of ion trajectories from ballistic ones are calculated. These calculations are taken into account to optimize the design of the reversible magnetic focusing system. The current density profile is obtained in the plane of the beam crossover. It demonstrates the high power density localization up to 3 kW/cm^2. This ion-beam system optimization is applicable for high-speed

etching, polishing and deposition of thin films [5] using single dc power supply.

This work investigates also the trimming process that uses FALCON ion source for high-precision adjustment of the thickness of functional microelectronics layers. The non-uniform layers deposited on the wafer are etched by scanning focused ion beam, which spatial positioning and power correspond to the topography of layer non-uniformity.

Experimental techniques and results

The experiments were performed using the ion beam trimming installation for high-precision adjustment of the thickness of functional microelectronics layers that utilizes the wafers with a diameter of 100÷200 mm (see Fig. 1). The system was mounted inside the vacuum chamber (1) that provides the residual pressure of 10^{-7} Torr (working pressure is 10^{-5} Torr) with the use of turbomolecular pump. The ion-beam system consisted of ion source generating the ion beams of the keV range (2), and coordinate system for the positioning and scanning (3, 4). The coordinate system was controlled through the specialized software and allows precise local etching of the material.

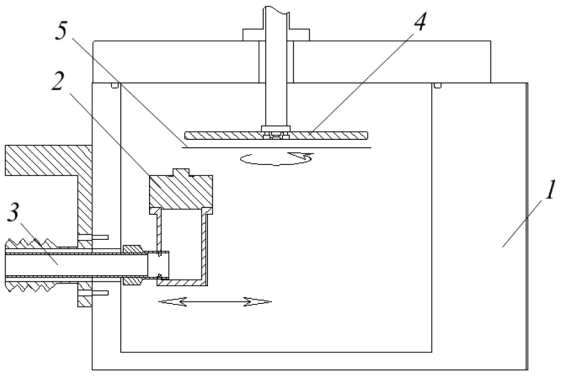

Fig. 1. The scheme of the ion-beam trimming system: 1 – vacuum chamber, 2 – ion beam source, 3 – coordinating system, 4 – spinning wafer holder, 5 – processing wafer.

Fig. 1 shows the scheme of the trimming device, where the positioning is implemented using 2-D polar coordinates. The implementation of the positioning system using Cartesian coordinate system was also possible.

The surface was treated by small-sized Hall-type ion beam source (Fig. 2) designed to provide the ballistic and magnetic focusing of the ion beam [1].

Fig. 2. The ion source used for trimming and the focused ion beam.

If the method of ballistic focusing is used for enhancing the beam current density then the theoretical geometric coefficient of compression is equal (see Fig. 3.):

$$G_j = \frac{8R\sin^2\alpha}{a}. \qquad (1)$$

For the geometric values which are typical for our experimental conditions, the coefficient of compression is equal $G_j = 171$.

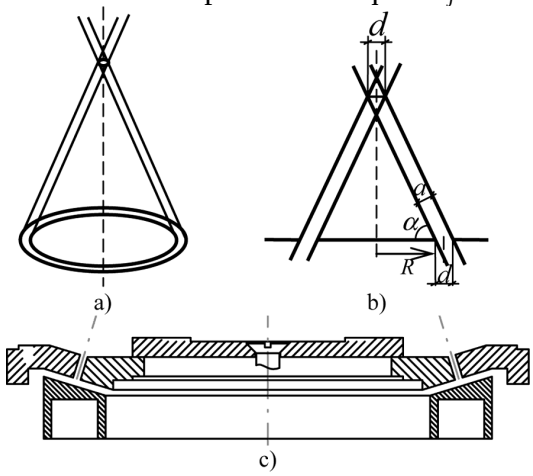

Fig. 3. Model of the beam ballistic focusing (a), its geometric parameters (b), developed hardware (c).

The area of the crossover was expected to be $S(crossover) = 3{,}45\ mm^2$. The used beam current is up to 200 mA while the average ion energy is 1 keV in the commercial Hall thruster. Via decreasing the square of the beam cross-section we expected to get the beam density $j_{crossover}$=5,79 A/cm^2 and rather high power density $P = j\,\varepsilon_{ib}$=116 MW/m^2, where ε_{ib} is ion kinetic energy.

To realize the ballistic focusing usual plane cathode and anode were replaced by the new units of special shape (Fig. 3(c)) with

channels which provide the producing of cone-like beam (Fig. 2).

Minimum diameter of the beam in the plane of crossover obtained due to the utilization of ballistic focusing reached 1.5 cm. Thus the ballistic focusing itself did not produce ideal cone-like beam in the Hall source.

Overall deviation of the ion trajectory from the dot of focus is given by the following expression:

$$y_\Sigma = \frac{\omega_{c1} l_1^2}{2\upsilon_0} + \frac{\omega_{c1} l_1 L}{\upsilon_0} = \frac{l_1 L}{\rho_L} \sim \frac{B}{\sqrt{U}}. \qquad (2)$$

In (2), ω_{c1} is ion gyrofrequency caused by magnetic field within ballistic focusing gap, l_1 is the length of magnetic field of ballistic focusing, υ_0 is ion velocity caused by discharge voltage, L is the distance without magnetic field from ballistic focusing electrodes to crossover region, ρ_L is the ion gyroradius, B is magnetic induction, U is discharge voltage.

The expression (2) shows the main problem, videlicet, the transversal pulse obtained by the ion at the short distance l_1 retains the same at the long distance L. To improve the focusing it was proposed to compensate the transversal pulse by the magnetic field of opposite direction, i.e. to use the magnetic system with reversible magnetic field in the Hall ion source.

To find out the trajectories of the ions in the Hall ion source with the ballistic and magnetic focusing analogue of the Bush theorem for paraxial beams [6] and the energy conservation law were used:

$$m\dot{x} - m\dot{x}_0 = -e(\psi - \psi_0), \qquad (3)$$

$$\frac{m\dot{x}^2}{2} - \frac{m\dot{y}^2}{2} = \varepsilon_i = \frac{m\upsilon_0^2}{2}. \qquad (4)$$

Here m is ion mass, x is transverse ion coordinate, x_0 is initial ion coordinate, e is elementary charge, ψ is magnetic field flux, ψ_0 is initial magnetic field flux, ε_i is ion kinetic energy.

It is possible to derive from eqs. (3) and (4) the expressions for the ions trajectories within three consistent areas particles are moving through (Fig. 4). The first area is the magnetic field of ballistic focusing. In the second area, a particle moves in the reverse magnetic field produced by the magnetic circuits of magnetic focusing. The third area is the beam drift region almost without magnetic field where the particles move according to the previously acquired pulses.

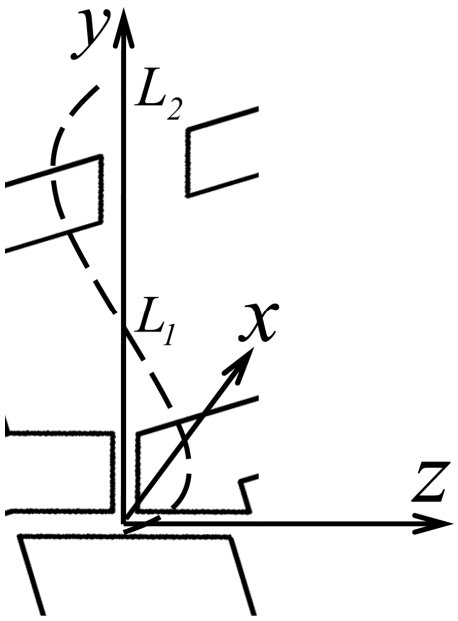

Fig. 4. Qualitative distribution of the magnetic field in the magnetic conductors system.

Ion trajectory within the first area, $0<y<L_1$, is described by the following expression:

$$x(y) = \sqrt{\frac{\upsilon_0^2}{\omega_{c1}^2}} - \sqrt{\frac{\upsilon_0^2}{\omega_{c1}^2} - y^2}. \qquad (5)$$

For the second area, $L_1<y<L_2$, ion trajectory is as follows:

$$x(y) = \frac{1}{\omega_{c2}}\left\{\sqrt{\upsilon_0^2 - [(\omega_{c1}+\omega_{c2})L_1 - \omega_{c2}y]^2} - \right.$$

$$\left. - \sqrt{\upsilon_0^2 - \omega_{c1}^2 L_1^2}\right\} + \sqrt{\frac{\upsilon_0^2}{\omega_{c1}^2}} - \sqrt{\frac{\upsilon_0^2}{\omega_{c1}^2} - L_1^2}. \qquad (6)$$

Here ω_{c2} is ion gyrofrequency caused by magnetic field within magnetic focusing area.

And for the third area, $L_2<y<L_3$, one can obtain:

$$x(y) = \frac{\omega_{c1}L_1 + \omega_{c2}(L_2 - L_1)}{\sqrt{\upsilon_0^2 + \omega_{c2}^2(L_2 - L_1)^2}}(y - L_2) +$$

$$+ \frac{1}{\omega_{c2}}\left\{\sqrt{\upsilon_0^2 - [(\omega_{c1}+\omega_{c2})L_1 - \omega_{c2}L_2]^2} - \right.$$

$$\left. - \sqrt{\upsilon_0^2 - \omega_{c1}^2 L_1^2}\right\} + \sqrt{\frac{\upsilon_0^2}{\omega_{c1}^2}} - \sqrt{\frac{\upsilon_0^2}{\omega_{c1}^2} - L_1^2}. \qquad (7)$$

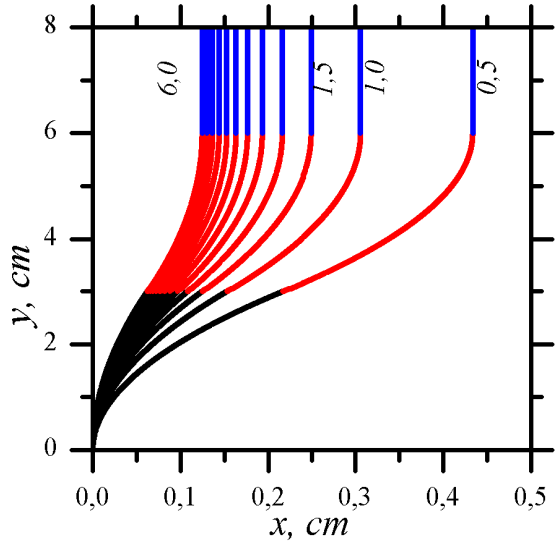

Fig. 5. The Ar ions trajectories in focused Hall thruster. Curve marked with “0.5” corresponds to the 0.5 keV ion trajectory and “6.0” - to the 6 keV.

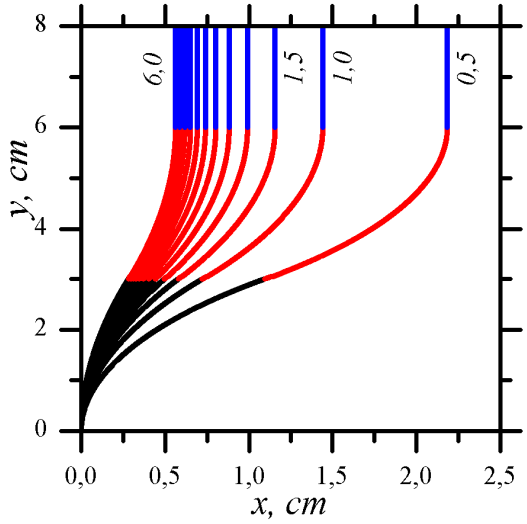

Fig. 6. The H ions trajectories in focused Hall thruster. Curve marked with “0.5” corresponds to the 0.5 keV ion trajectory and “6.0” - to the 6 keV.

The trajectories of argon and hydrogen ions in focused Hall thruster are shown in Fig. 5 and 6.

It is possible to adjust beam focusing via varying the ratio of magnetic field fluxes in gaps of the magnetic conductors and varying the lengths of the first and second areas.

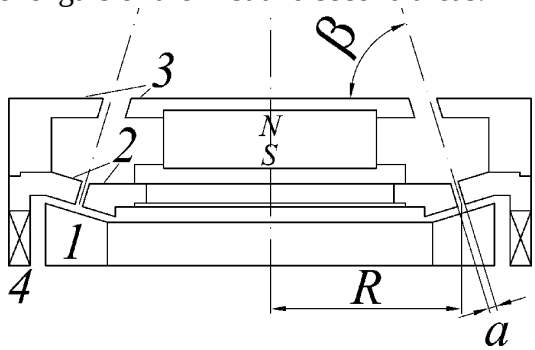

Fig. 7. Hall ion source with the ballistic and magnetic beam focusing: 1 – anode, 2 – cathode-magnetic conductor providing the ballistic focusing, 3 – magnetic focusing electrode, 4 – magnetic field coil.

The additional magnetic conductor (indicated with “3” in Fig. 7) was placed on the ballistic focusing electrodes (indicated with “2” in Fig. 7) to realize magnetic beam focusing. This additional magnetic conductor provided the magnetic field of opposite direction in respect of the field in the discharge gap of the source. Magnetic field coil served to align the magnetic flux along the ballistic trajectory of the ion beam and to reach the minimum beam diameter in the plane of the crossover.

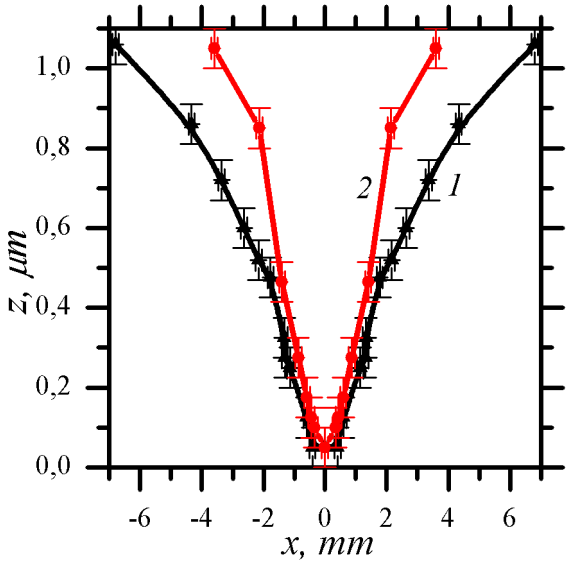

Fig. 8. The ion beam intensity, obtained by sputtering of the SiO_2 layer with Ar (1) ion beam and H (2) ion beam.

The profile of the ion beam intensity was measured via etching the *SiO_2* layers. These layers are of different colours for different layer thicknesses. Fig. 8 shows the ion beam intensity, obtained by sputtering the *SiO_2* layer with *Ar* ion beam (beam current was of *40 mA* and average ion energy was of *1 keV*) and *H* ion beam (beam current was of *10 mA* and average ion energy was of *1 keV*). One can see that the beam intensity is well concentrated within the diameter of *4 mm*.

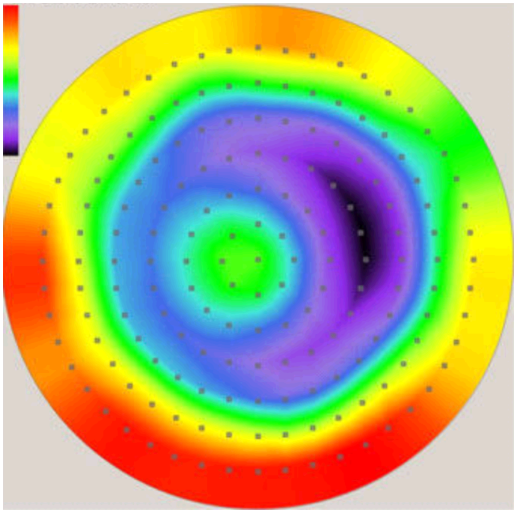

Fig. 9. Typical topography of non-uniformity of the AlN layer obtained by magnetron deposition. The gray dots show the points, where the layer thickness has been measured.

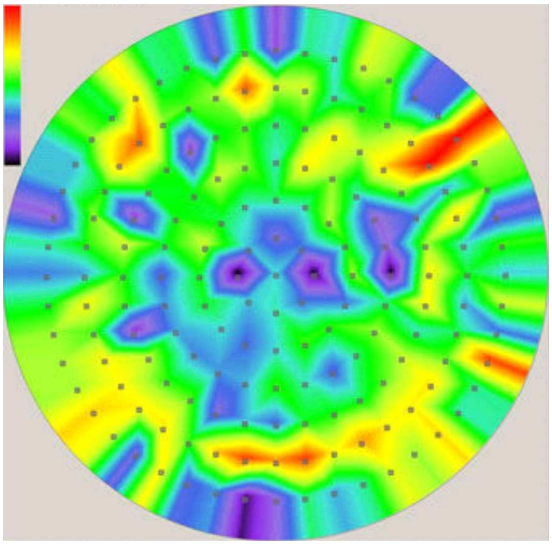

Fig. 10. Typical topography of the non-uniformity measured for the AlN layer after the single pass trimming with Ar ion beam.

The ion source generated conical beam of *Ar* ions with energy of *300÷1500 eV* and current of *1÷50 mA* during the trimming experiments. The increase of the ion beam current density in comparison to cylindrical one is described by coefficient of the beam compression. For the ion source used for the trimming the compression coefficient was about *50*.

The local etching rate of the functional layers was regulated by varying the power of the beam. The gas discharge power in Hall-type ion source with anode layer can be easily controlled by varying the voltage applied to the anode. In the trimming tool (Fig. 1), software controls the positioning mechanism and the voltage of the discharge.

The investigation of surface polishing by trimming was carried out using the *Si* wafers with a diameter of *150 mm* with *AlN* layer. The layer thickness was *1÷1.5* micrometers and it was deposited by magnetron physical sputtering.

The process of the ion beam polishing consists of two stages. At first, the triradial interferometer measures the thickness of the layer at a number of points. The number of measurement points can be varied up to *1000*, however, typical number of the points corresponds to number of chips manufactured on the wafer. The topography of the functional microelectronics layer is produced by software basing on the results of measurements. The topography map is used then to calculate the parameters of the topography correction: the position of the ion source and its discharge power. For example, Fig. 9 shows typical topography of the aluminium nitride layer deposited by magnetron sputtering. The parameters of the topography are as follows: average layer thickness is *8265.4 Å*; maximum thickness is *8341.7 Å*; minimum thickness is *8179.8 Å*; the data spread for the layer thickness is *161.8 Å*.

The topography of the layer would differ only slightly if the batch of *Si* wafers with aluminium nitride deposition are produced in the same manufacturing process. Therefore, one can use average parameters of the topography for the trimming of the whole batch of the samples.

After measurement of the topography, the functional layer was etched by the trimming, i.e. it was exposed to the scanning ion beam. The position and the power of the ion beam were controlled by the software, which set the trimming parameters according to measured map of the layer topography. Following the trimming process, the topography of the layer was measured once more in the same way. Fig. 10 shows typical topography of the layer non-uniformity, obtained after the single pass trimming process. The parameters of the topography, obtained in this particular case, are as follows: average layer thickness is *8172.3 Å*; maximum thickness is *8176.2 Å*; minimum thickness is *8169.0 Å*; the data spread of the layer thickness is *7.2 Å*.

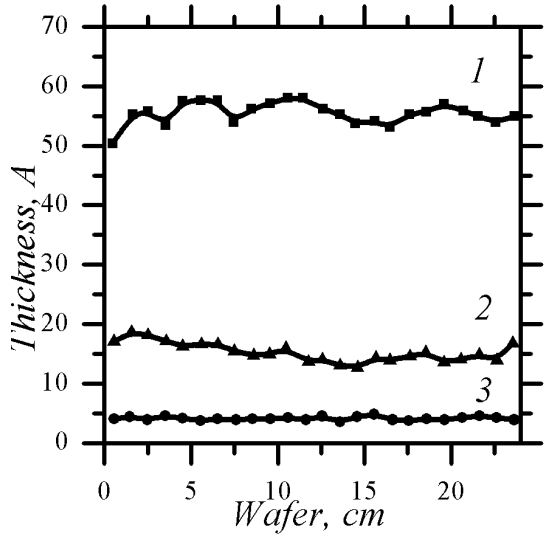

Fig. 11. Functional layer uniformity: 1 – as deposited, 2 – after the first trim based on monitor wafer map; 3 – after the second trim, based on individual maps.

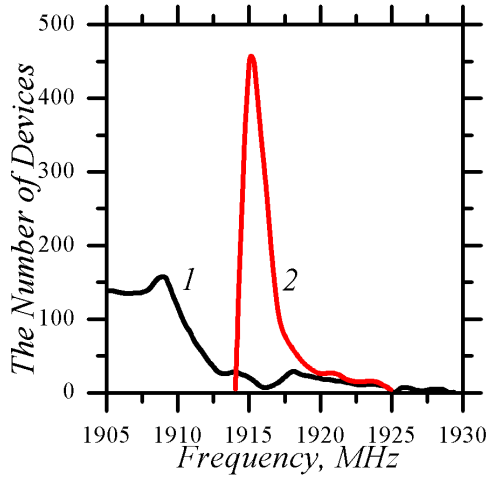

Fig. 12. Distribution of number of the FBAR chips obtained from the same wafer as a function of their working frequency: 1 – initial; 2 – after single trimming.

The Fig. 11 demonstrates the uniformity of functional layer and its improvement in the result of two trimming stages. The curve “1” shows the thickness of the initial deposited layer. The curve “2” shows the thickness of the layer after it was processed for the first time on the base of monitor wafer map. The curve “3” corresponds to the results of the second trim of the layer based on the individual map. It is proved that intellectual trimming based on individual map strongly decreases the non-uniformity of the *AlN* layer down to sub-nanometer scale over the surface of diameter of *150 mm*. The obtained layer can be used as FBAR, which thickness value defines the acoustic frequency, generated by FBAR.

Fig. 12 shows the distribution of the number of FBAR chips, obtained from the same wafer, as a function of their working frequency. One can see that chips obtained from the wafer, that has not been processed with the trimming, have wider distribution of the working frequencies ranging from *1905 MHz* to *1930 MHz*. In contrast, the working frequency of the chips obtained from the trimmed wafer is located mostly around the value of *1916 MHz*. Narrower distribution of the chip frequencies increases the chip yield per wafer, decreasing their prime cost and increasing, therefore, the overall economical efficiency of the chip manufacturing.

Conclusions

This paper describes the important application of the FALCON ion source, which demonstrates both technological advances and economical efficiency of the trimming process.

The deviations of ion trajectories from ballistic ones in FALCON ion source are calculated. These calculations are taken into account to optimize the design of the reversible magnetic focusing system. The current density profile is measured in the plane of the beam crossover. It demonstrates the high power density localization up to *3 kW/cm*^{2}.

The ion beam etching for high-precision adjustment of the thickness of functional microelectronics layers is investigated. The topography (i.e. local thickness) of layer deposited on the substrate is measured and these measurements are used for controlling the layer processing by scanning focused ion beam. Its spatial positioning and ion beam power is controlled accordingly to the topography through the software. The trimming allows production of pre-defined topography of the layer with the thickness spread down to *4 Å*. Experiments show that the surface roughness can be decreased down to sub-nanometer scale. As the result, the trimming process provides the increased chip yield and, correspondingly, increased economic efficiency of the overall production process.

СПИСОК ВИКОРИСТАНОЇ ЛІТЕРАТУРИ

1. Brown I.G. The Physics and Technology of Ion Sources (WILEY-VCH Verlag GmbH & Co. KGaA, Weinheim, 2004).
2. Zhurin V.V., Kaufman H.R., Robinson R.S. Plasma Sources Sci. Technol., 8, R1 (1999).
3. Gutkin M., Bizyukov A., Sleptsov V., Bizyukov I., Sereda K., U.S. Patent #US 7,622,721 B2, 2008/0191629 A1.
4. Bizyukov A.A., Girka A.I., Sereda K.N., Nazarov A.V., Romaschenko E.V. Problems of Atomic Science and Technology, № 6, Series: Plasma Physics, 174 (2008).
5. Danilin B.S., Kireev V.Yu. The application of low-temperature plasmas for materials etching and cleaning (Energoatomizdat, Moskov, 1987) (in Russian).
6. Molokovskiy S.I., Sushkov A.D. Intensive electron and ion beams (Energija, Leningrad, 1972) (in Russian).

Стаття надійшла до редакції 27.05.2011

О.І. Гірка[1], І.О. Бізюков[1], О.А. Бізюков[1],
К.М. Середа[1], О.В. Ромащенко[2]
[1] Харківський національний університет ім. В.Н.Каразіна, 61022, Харків, пл. Свободи, 4
[2] Східноукраїнський національний університет ім. В.І. Даля,
91034, Луганськ, Молодіжний квартал, 20-А

СФОКУСОВАНЕ ДЖЕРЕЛО ІОНІВ ДЛЯ ОБРОБКИ ТОНКИХ ПЛІВОК МІКРОЕЛЕКТРОНІКИ

У роботі показано результати застосування оптимізованого компактного іонного джерела для коригуючого іонно-променевого травлення для регулювання товщини функціональних шарів мікроелектроніки з високою точністю. Функціональний шар на підкладці витравлюється скануючим сфокусованим іонним пучком, локалізація та потужність якого відповідає топографії неоднорідності товщини функціонального шару. Показано можливість регулювання розподілу товщини плівок по поверхні підкладок до +/–4 Å та зменшення шорсткості поверхні.
Ключові слова: компактне іонне джерело, топографія, товщини функціонального

А.И. Гирка[1], И.О. Бизюков[1], О.А. Бизюков[1],
К.Н. Середа[1], Е.В. Ромащенко[2]
[1]Харьковский национальный университет им. В.Н. Каразина
61022, Харьков, пл. Свободы 4, Украина
[2] Восточноукраинский национальный университет им. В.И. Даля
91034, Луганск, Молодежный квартал, 20-А, Украина

СФОКУСИРОВАННЫЙ ИСТОЧНИК ИОНОВ ДЛЯ ОБРАБОТКИ ТОНКИХ ПЛЕНОК МИКРОЭЛЕКТРОНИКИ

В работе представлены результаты применения оптимизированного компактного источника ионов для корректирующего ионно-лучевого травления для регулирования толщины функциональных слоёв микроэлектроники с высокой точностью. Функциональный слой на подложке протравливается сканирующим сфокусированным ионным пучком, локализация и мощность которого соответствует топографии неоднородности толщины функционального слоя. Показана возможность регулировки распределения толщины пленок по поверхности подложек и уменьшения шероховатости поверхности до 4 Å.
Ключевые слова: компактный источник ионов, баллистическая и магнитная фокусировка пучка, неоднородность функционального слоя, ионно-лучевое травление.